The epithelial Ca^{2+} channel TRPV5 is essential for proper osteoclastic bone resorption

Bram C. J. van der Eerden*, Joost G. J. Hoenderop†, Teun J. de Vries‡, Ton Schoenmaker‡, Cok J. Buurman*, André G. Uitterlinden*, Huibert A. P. Pols*, René J. M. Bindels†, and Johannes P. T. M. van Leeuwen*§

*Department of Internal Medicine, Erasmus Medical Center, 3000 DR, Rotterdam, The Netherlands; †Department of Physiology, Nijmegen Centre for Molecular Life Sciences, Radboud University Nijmegen Medical Centre, 6500 HC, Nijmegen, The Netherlands; and ‡Department of Periodontology, Oral Cell Biology, Academic Centre of Dentistry Amsterdam, Universiteit van Amsterdam and Vrije Universiteit, 1081 HV, Amsterdam, The Netherlands

Edited by Hector F. DeLuca, University of Wisconsin, Madison, WI, and approved October 10, 2005 (received for review July 11, 2005)

Bone remodeling involves the interplay of bone resorption and formation and is accurately controlled to maintain bone mass. Both processes require transcellular Ca^{2+} transport, but the molecular mechanisms engaged remain largely elusive. The epithelial Ca^{2+} channel TRPV5 is one of the most Ca^{2+}-selective transient receptor potential (TRP) channels. In this study, the functional role of TRPV5 in bone was investigated. TRPV5 mRNA was expressed in human and murine bone samples and in osteoclasts along with other genes involved in transcellular Ca^{2+} transport, including calbindin-D_{9K} and calbindin-D_{28K}, Na^+/Ca^{2+} exchanger 1, and plasma membrane Ca^{2+}-ATPase 1b. TRPV5 expression in murine osteoclasts was confirmed by immunostaining and showed predominant localization to the ruffled border membrane. However, TRPV5 was absent in osteoblasts. Analyses of femoral bone sections from TRPV5 knockout ($TRPV5^{-/-}$) mice revealed increased osteoclast numbers and osteoclast area, whereas the urinary bone resorption marker deoxypyridinoline was reduced compared with WT ($TRPV5^{+/+}$) mice. In an *in vitro* bone marrow culture system, the amount of osteoclasts and number of nuclei per osteoclast were significantly elevated in $TRPV5^{-/-}$ compared with $TRPV5^{+/+}$ mice. However, using a functional resorption pit assay, we found that bone resorption was nearly absent in osteoclast cultures from $TRPV5^{-/-}$ mice, supporting the impaired resorption observed *in vivo*. In conclusion, TRPV5 deficiency leads to an increase in osteoclast size and number, in which Ca^{2+} resorption is nonfunctional. This report identifies TRPV5 as an epithelial Ca^{2+} channel that is essential for osteoclastic bone resorption and demonstrates the significance of transcellular Ca^{2+} transport in osteoclastic function.

tartrate-resistant acid phosphatase | $1,25(OH)_2D_3$ | osteoblast | Coomassie blue | laser scanning confocal microscopy

Maintenance of body Ca^{2+} is of crucial importance for many physiological functions, including neuronal excitability, muscle contraction, and bone formation. Bone is the major Ca^{2+} storage of the body and regulates in concerted action with kidney and intestine the whole-body Ca^{2+} balance. Transcellular Ca^{2+} transport is an important process in maintaining Ca^{2+} balance by these tissues (1, 2). In bone, it is crucial for bone formation/mineralization to achieve adequate bone quality and strength, but also for osteoclastic bone resorption, which contributes to Ca^{2+} balance in the blood. However, the proteins involved in transcellular Ca^{2+} transport in bone cells are largely elusive. Recently, TRPV5 and TRPV6, members of the superfamily of transient receptor potential (TRP) cation channels, have been identified as the gatekeepers of transepithelial Ca^{2+} transport in kidney and intestine, respectively (3–5). These highly selective epithelial Ca^{2+} channels are part of a three-step process, facilitating transcellular Ca^{2+} transport (3, 4, 6). After entry of Ca^{2+} into the cell through TRPV5 and TRPV6, Ca^{2+} bound to calbindin-D_{28K} and/or calbindin-D_{9K} diffuses to the basolateral membrane. There, Ca^{2+} is extruded via Na^+/Ca^{2+} exchanger 1 (NCX1) and ATP-dependent plasma membrane Ca^{2+}-ATPase 1b (PMCA1b). In a recent study, we generated mice lacking TRPV5 ($TRPV5^{-/-}$), which displayed severe renal Ca^{2+} wasting and compensatory intestinal hyperabsorption of Ca^{2+}. Moreover, the knockout mice exhibited significant disturbances in bone structure, including reduced femoral cortical and trabecular bone thickness (7).

Those findings prompted us to investigate the role of TRPV5 in bone. First, the expression of TRPV5 and the other transcellular Ca^{2+} transporters in bone cells was studied by real-time PCR analysis and immunocytochemistry. Second, bone resorption was measured in urine, and histological analyses were carried out on femoral bones from WT mice ($TRPV5^{+/+}$) and $TRPV5^{-/-}$ mice. Finally, a series of bone marrow culture experiments and bone resorption assays were performed to investigate the role of TRPV5, demonstrating that in mice lacking the epithelial Ca^{2+} channel TRPV5 bone resorption is impaired despite enhanced osteoclastogenesis. These studies exhibit an important role for TRPV5 and transcellular Ca^{2+} transport in bone resorption.

Materials and Methods

Human Femoral Head Biopsy and Mouse Femurs. Human bone material was obtained from femoral head biopsies of osteathritic bone. This material was collected within a clinical study, which was approved by the local medical ethical commission. Furthermore, three mice (strain B6.129) were killed to collect femurs, from which the bone marrow was flushed. The remaining bone sample was then homogenized with a Mikro Dismembrator S (Sartorius). The resulting powder was further processed for RNA isolation as described below.

Human and Murine Osteoclast Cultures. Buffy coats were obtained from healthy donors and diluted 1:1 with Hank's buffered salt solution (HBSS). Twenty milliliters of diluted peripheral blood mononuclear cells (PBMCs) was layered onto 15 ml of Lymphoprep (1.077 ± 0.001 g/liter; Axis-Shield Po CAS, Oslo) and centrifuged at 1,200 × *g* for 30 min at room temperature. PBMCs were recovered from the interface and washed twice with HBSS supplemented with 2% (vol/vol) FCS. Monocytes were isolated from the PBMCs by separation on a Percoll gradient (Amersham Pharmacia) consisting of three density layers (1.076, 1.059, and 1.045 g/ml). The fraction present in the middle layer, which contained predominantly monocytes, was seeded in 96-well culture plates at a density of 10^5 cells per well and cultured for 3 weeks in DMEM supplemented with 10% (vol/vol) FCS and 1% (vol/vol) antibiotic-antimyotic solution containing 30 ng/ml human macrophage-colony-stimulating factor (M-CSF; R & D Systems) and 20

Conflict of interest statement: No conflicts declared.

This paper was submitted directly (Track II) to the PNAS office.

Abbreviations: TRP, transient receptor potential; NCX1, Na^+/Ca^{2+} exchanger 1; PMCA1b, plasma membrane Ca^{2+}-ATPase 1b; M-CSF, macrophage-colony-stimulating factor; TRACP, tartrate-resistant acid phosphatase; ALP, alkaline phosphatase; DPD, deoxypyridinoline; PBMC, peripheral blood mononuclear cell; RANKL, human receptor-activated NF-κB.

§To whom correspondence should be addressed. E-mail: j.vanleeuwen@erasmusmc.nl.

Table 1. Sequences of primers and Taqman probes for real-time PCR

Gene	Species	Forward primer	Reverse primer	Probe
HPRT	M	TTATCAGACTGAAGAGCTACTGTAATGATC	TTACCAGTGTCAATTATATCTTCAACAATC	TGAGAGATCATCTCCACCAATAACTTTTATGTCCC
GAPDH	H	ATGGGGAAGGTGAAGGTCG	TAAAAGCAGCCCTGGTGACC	CGCCCAATACGACCAAATCCGTTGAC
TRPV5	M	CGTTGGTTCTTACGGGTTGAAC	GTTTGGAGAACCACAGAGCCTCTA	TGTTTCTCAGATAGCTGCTCTTGTACTTCCTCTTTGT
	H	TTGCCTCCGCGTTCTATATCA	GGCAAGTCCACGTCGTAGTTG	ACTACCCCATGGCACTGTTCACCACC
CaBP-D_{9K}	M	CCTGCAGAAATGAAGAGCATTTT	CTCCATCGCCATTCTTATCCA	CAAAAATATGCAGCCAAGGAAGGCGA
	H	AATGAGTACTAAAAGTCTCCTGAGGAACT	AGGGTGTTTGGACCTTTGAGTAAA	TCTGGATCACCTTCTTTGGCTGCATATTTTTC
CaBP-D_{28K}	M	AACTGACAGAGATGGCCAGGTTA	TGAACTCTTTCCCACACATTTTGAT	ACCAGTGCAGGAAAATTTCCTTCTTAAATTCCA
	H	CCTAATGCTGAAACTATTTGATTCAAATAA	TCTTTCCCACACATTTTGATTCC	CCAGGTTACTACCAGTGCAGGAGAATTTTCTTCTTAA
NCX1	M	TCCCTACAAAACTATTGAAGGCACA	TTTCTCATACTCCTCGTCATCGATT	ACCTTGACTGATATTGTTTTGACTATTTCATCATTCTGGA
	H	CAAAACAATATCAGTCAAGGTAATTGATG	CCTCACGGTCAAATATTCTAATGGT	AAGACCTTCTTCCTTGAGATTGGAGAGCCC
PMCA1	M	CGCCATCTTCTGCACCATT	CAGCCATTGCTCTATTGAAAGTTC	CAGCTGAAAGGCTTCCCGCCAAA
	H	CAACAATTCCAACTAGCCGTTTAA	GGCCACGCCGCAACT	CCTTTTGTGTTCCATGACCAGCTTCTTTGA

PCR primers and fluorescent probes (5′-6-carboxyfluorescein- and 3′-6-carboxytetramethylrhodamin-labeled) were designed by using the computer program PRIMER EXPRESS (version 1.5; Applied Biosystems) and were purchased from Applied Biosystems (GAPDH), Eurogentec (other human sequences), or Biolegio (Malden, The Netherlands) (mouse sequences). HPRT, hypoxantine-guanine phosphoribosyl transferase; TRPV5, transient receptor potential channel V5; CaBP, calbindin; M, murine; H, human.

ng/ml human receptor-activated NF-κB (RANKL; PeproTech London). The media were refreshed twice a week.

Culturing murine bone marrow cells has been described (8). Cells were cultured for 6 days in the presence of 30 ng/ml recombinant M-CSF (R & D Systems) and 20 ng/ml recombinant murine RANKL-TEC (R & D Systems), and the media were refreshed at day 3. At the end of the human and murine cultures, cells were washed with PBS, fixed in PBS-buffered paraformaldehyde (4% vol/vol) or formalin (10% vol/vol), respectively, and stored at 4°C for tartrate-resistant acid phosphatase (TRACP) staining and immunocytochemistry. Alternatively, murine osteoclasts cultured on bovine cortical bone slices were lysed in water for Coomassie brilliant blue staining of resorption pits (8).

Murine Osteoblast Cultures. Bone marrow cells were collected as described (8). Cells were cultured in phenol-red free α-minimal essential medium (GIBCO/BRL), supplemented with 100 units/ml penicillin, 100 μg/ml streptomycin (Life Technologies, Breda, The Netherlands), 250 ng/ml amphotericin B (Sigma), 20 mM Hepes, 1.8 mM $CaCl_2$, and 15% (vol/vol) heat-inactivated FCS (GIBCO/BRL), pH 7.5. From day 3 onward, the culture medium was supplemented with 50 μM vitamin C (Sigma) and 10 mM β-glycerophosphate (Sigma). At days 10 and 20 of culture cells were fixed in 70% ethanol and stained for alkaline phosphatase (ALP) and alizarin red, respectively. For ALP staining, cells were incubated in Tris·HCL (pH 9.5) containing 50 mM $MgCl_2$, 0.6 mg/ml bromo-chloro-indoryl phosphate (Sigma), and 150 μg/ml nitro blue tetrazolium (Sigma) for 20 min and washed with PBS. Alizarin red staining was performed, incubating the cells for 10 min in a saturated alizarin red S solution in distilled water (pH 4.2), after which the cells were washed with distilled water. The number of ALP- and alizarine red-positive colonies was counted with a microscope.

Collection of Femurs, Serum, and Urine. From 8-week-old male and female TRPV5$^{+/+}$ and TRPV5$^{-/-}$ mice, femurs (n = 9) were prepared and routinely processed for plastic embedding (9), and 10-μm sections were cut. Urine was collected, and total deoxypyridinoline (DPD) cross-links were determined with the Metra DPD assay (Quidel, San Diego).

RNA Isolation, cDNA Synthesis, and Real-Time PCR. The pulverized material from the human femoral head biopsy and mouse femurs was resuspended in RNA-Bee solution (Tel-Test, Friendswood, TX), and total RNA was isolated according to the manufacturer's protocol. Human (21 days) and murine (6 days) osteoclasts were dissolved in RNA lysis buffer from the RNeasy Mini Kit (Qiagen, Hilden, Germany). RNA isolation and cDNA synthesis were performed as described (10). Expression levels of TRPV5, calbindin-D_{9K}, calbindin-D_{28K}, NCX1, and PMCA1b were quantified by real-time PCR with an Applied Biosystems Prism 7700 sequence

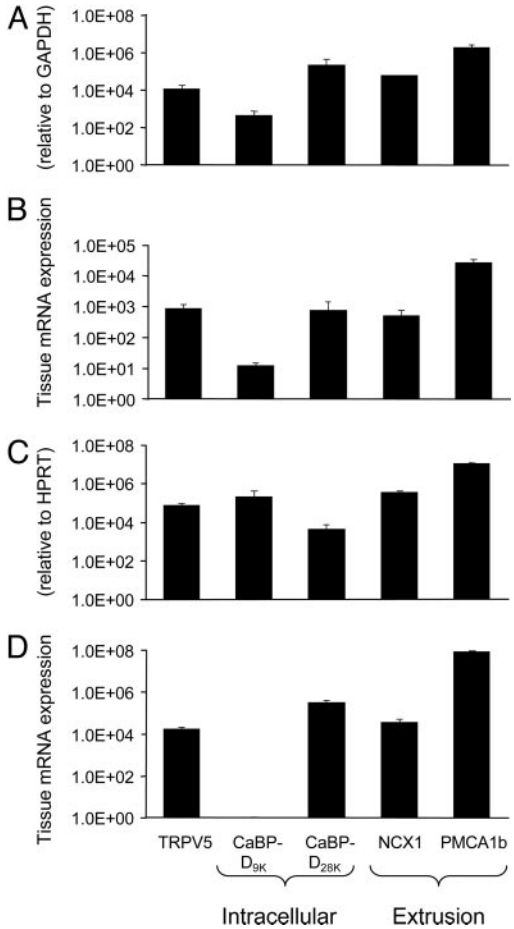

Fig. 1. TRPV5 is expressed in human and murine osteoclasts. Total RNA was isolated from human femoral biopsy samples (*A*), human PBMC-derived osteoclast-like cells (*B*), murine femurs (*C*), and osteoclasts derived from murine tibial bone marrow cultures (*D*). The mRNA expression of TRPV5, the intracellular Ca^{2+} binding proteins calbindin-D_{9K} (CaBP-D_{9K}) and calbindin-D_{28K} (CaBP-D_{28K}), and the Ca^{2+} extrusion proteins NCX1 and PMCA1b was measured. The accolades refer to the supposed function of the different genes: TRPV5 for uptake of Ca^{2+}, the calbindins for intracellular Ca^{2+} transport, and NCX1 and PMCA1b for extrusion of Ca^{2+}. HPRT, hypoxanthine-guanine phopshoribosyl transferase.

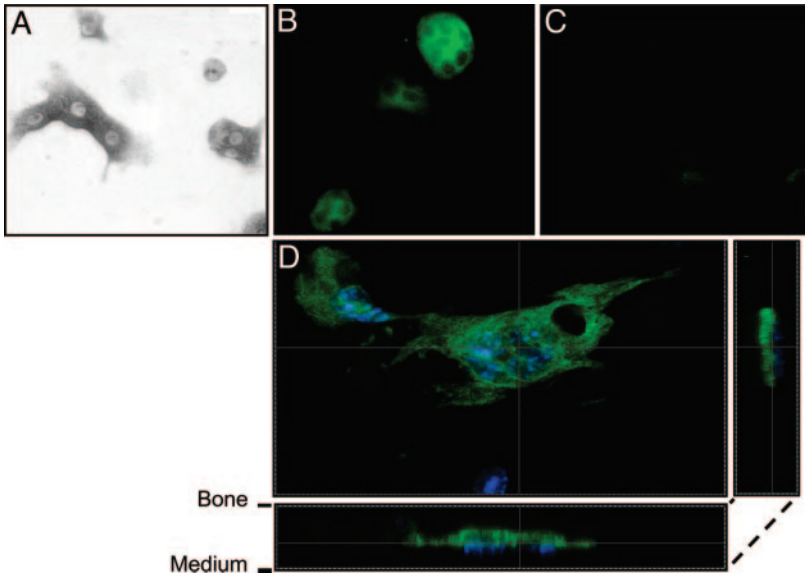

Fig. 2. TRPV5 is predominantly visualized in the ruffled border membrane of murine osteoclasts. Murine osteoclasts derived from bone marrow were cultured on bone slices in the presence of M-CSF and RANKL for 6 days. (*A*) Osteoclasts were identified by TRACP staining. (*B* and *C*) TRPV5 staining (green) was demonstrated in osteoclasts derived from TRPV5$^{+/+}$ mice (*B*) but not from TRPV5$^{-/-}$ mice (*C*). (*D*) Confocal laser scanning microscopy showed TRPV5 staining predominantly at the ruffled border membrane, where bone resorption occurs. Nuclei are stained with DAPI (blue).

detection system. The expression of human GAPDH and murine hypoxanthine-guanine phopshoribosyl transferase was used as an internal control to normalize for differences in RNA extraction and degradation and for efficiency of the cDNA synthesis. The different primers and 5′-6-carboxyfluorescein-3′-6-carboxytetramethylrhodamin-labeled probes (Eurogentec, Seraing, Belgium) (Table 1) for the genes of interest were designed with PRIMER EXPRESS software (Applied Biosystems). Data are presented as relative mRNA levels calculated by the formula: relative expression = $2^{\Delta}-$(Ct of gene of interest − Ct of household gene).

Immunocytochemistry. Murine osteoclasts were cultured as described above. Cells were fixed in 10% (vol/vol) formalin in PBS for 10 min. The cells were incubated in 50 mM NH_4Cl for 10 min at room temperature to reduce auto fluorescence and subsequently permeabilized with 0.1% (vol/vol) Triton X-100 for 5 min. Next, the cells were incubated in 0.2% (vol/vol) BSA in 1 × TBS (TBS/BSA) for 30 min followed by incubation with a polyclonal antibody raised in guinea pig directed against TRPV5 (GP3; 1:800) overnight at 4°C (11). The next day, cells were incubated with an Alexa Fluor 488 goat-anti-guinea pig antibody (Molecular Probes) at a dilution of 1:300 for 2 h at room temperature. Finally, the cells were washed in 1 × PBS and water and mounted in Vectashield containing DAPI (Vector Laboratories) for nuclear counterstaining. Pictures were taken with a Zeiss Axioplan 2 microscope. The murine osteoclast stainings were analyzed with a Leica DM IRB microscope or a Leica TCS-SP2 confocal laser scanning microscopy system (Leica Microsystems, Wetzlar, Germany). Negative controls included osteoclasts derived from TRPV5$^{-/-}$ bone marrow cultures.

TRACP Staining. Femoral bone sections were stained for TRACP, using 1.1 mM Naphtol AS-BI phosphate (Sigma) as substrate, 5.2 mM pararosanilin as coupler, and 46.5 mM sodium L-tartrate as inhibitor according to Scheven *et al.* (12). Fixed cells were stained for TRACP with an acid phosphatase leucocyte kit (Sigma) with small modifications. In particular, to visualize osteoclasts specifically, we used a 1 M tartrate solution instead of the supplied 0.33 M solution. The number of osteoclasts and nuclei per osteoclast were determined by two independent and blinded observers and with BIOQUANT NOVOPRIME digital-imaging software (Bioquant, Nashville, TN).

Resorption Pit Assay. Bovine cortical bone slices were sonicated in 10% (vol/vol) ammonia (Merck) for 10 min. After extensive washing, the cells were incubated in filtered potassium aluminum sulfate (Sigma) for 10 min and subsequently stained with filtered Coomassie brilliant blue (Phastgel Blue R; Amersham Pharmacia Biotech) for 5 s. The resorption pits were analyzed with BIOQUANT software.

Statistics. In all experiments values are expressed as mean ± SEM unless stated otherwise. Differences between groups were tested for significance by using the Student *t* test. Values were considered significantly different at $P < 0.05$.

Results and Discussion

The current study builds on our recent observations in the TRPV5$^{-/-}$ mice (7) and demonstrates the presence of TRPV5 in osteoclasts and its functional significance for osteoclastic bone resorption.

TRPV5 Is Expressed in Human and Murine Bone Samples and Osteoclasts. In two different human femoral head biopsies, TRPV5, calbindin-D_{9K}, calbindin-D_{28K}, NCX1, and PMCA1b mRNA were expressed (Fig. 1*A*). PBMC-derived human osteoclasts revealed mRNA transcripts for TRPV5, both calbindins, NCX1, and PMCA1b (Fig. 1*B*). In contrast, TRPV5 was not detected in human osteoblasts, whereas mRNAs for calbindin-D_{28K}, NCX1, and PMCA1b were expressed (data not shown). In the mouse femurs mRNAs encoding TRPV5 and the other Ca^{2+} transporters were detected (Fig. 1*C*). In bone marrow-derived murine osteoclasts, TRPV5 mRNA was coexpressed with calbindin-D_{28K}, NCX1, and PMCA1b mRNA, but calbindin-D_{9K} was not detected (Fig. 1*D*). As in human osteoblasts, TRPV5 mRNA was absent in cultured murine osteoblasts. Next, TRPV5 was investigated in murine osteoclasts by immunocytochemistry. Mouse tibial bone marrow cells treated with M-CSF and RANKL for 6 days and cultured on cortical bone slices showed TRACP-positive multinuclear osteoclasts (Fig. 2*A*). This finding was further substantiated by abundant expression of calcitonin receptor, which was absent in undifferentiated osteoclasts (data not shown). TRPV5 protein was evident in murine osteoclasts (Fig. 2*B*). The absence of signal in osteoclasts cultured from TRPV5$^{-/-}$ mice demonstrated the specificity of the TRPV5 staining (Fig. 2*C*). Assessment of TRPV5 immunocytochemistry by confocal laser scanning microscopy revealed that

PHYSIOLOGY

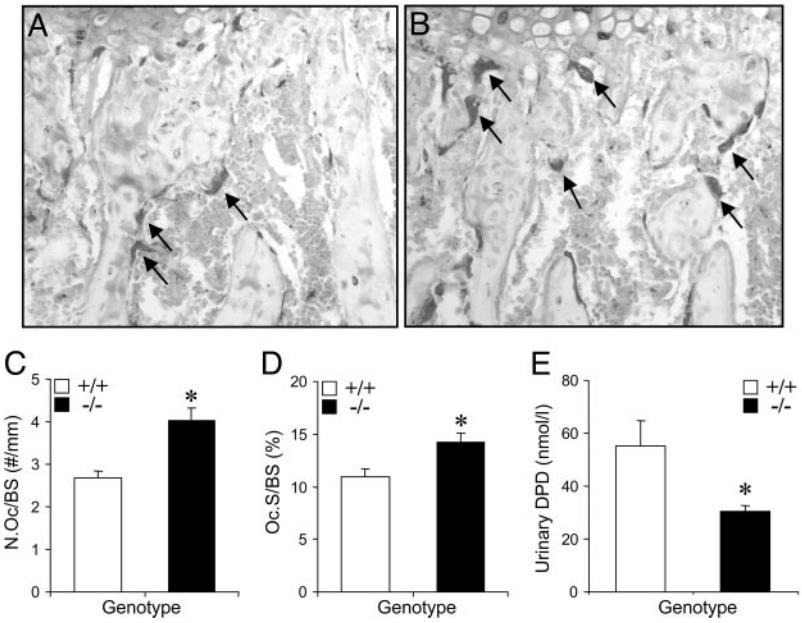

Fig. 3. TRPV5$^{-/-}$ mice exhibit enhanced osteoclastogenesis but reduced resorption. (*A* and *B*) TRACP staining was performed on femoral bone sections from TRPV5$^{+/+}$ (*A*) and TRPV5$^{-/-}$ (*B*) mice, and images were taken of the metaphyses. Arrows indicate osteoclasts. (*C* and *D*) Osteoclast number (*C*) and osteoclast surface area (*D*) per bone surface area was quantified ($n = 7$–8). (*E*) Urinary DPD levels were measured in TRPV5$^{+/+}$ and TRPV5$^{-/-}$ mice ($n = 9$). Values are presented as mean ± SEM. *, $P < 0.05$ versus TRPV5$^{+/+}$ mice.

TRPV5 staining is predominantly confined to the osteoclast ruffled border membrane (Fig. 2*D*). In summary, we demonstrated the presence of TRPV5 along with the other components of transcellular Ca^{2+} transport in osteoclasts, providing the means for transcellular Ca^{2+} transport analogous present in the kidney (3, 6, 7).

Osteoclastogenesis Is Enhanced and Bone Resorption Is Diminished in TRPV5$^{-/-}$ Mice. After its demonstration in osteoclasts, we investigated the role of TRPV5 in osteoclastogenesis and osteoclastic bone resorption *in vivo* and *in vitro*. First, we analyzed TRACP staining in the metaphyseal area of femoral bone sections derived from TRPV5$^{+/+}$ and TRPV5$^{-/-}$ mice. The number of TRACP-positive cells was increased in the TRPV5$^{-/-}$ mice compared with TRPV5$^{+/+}$ mice (Fig. 3 *A* and *B*). Quantification of the TRACP staining showed a significantly increased osteoclast number (Fig. 3*C*) and surface area (Fig. 3*D*) in the metaphysis of TRPV5$^{-/-}$ femurs. Surprisingly, urinary DPD levels were significantly reduced in TRPV5$^{-/-}$ mice compared with TRPV5$^{+/+}$ littermates (Fig. 3*E*). Taken together, these data demonstrated that bone resorption is reduced in TRPV5$^{-/-}$ mice, despite increased osteoclast number and size.

We further assessed the involvement of TRPV5 in osteoclast formation and function by culturing bone marrow cells from TRPV5$^{-/-}$ and TRPV5$^{+/+}$ mice with osteoclast-inducing cytokines M-CSF and RANKL. In cultures derived from TRPV5$^{-/-}$ mice, the number of osteoclasts was ≈2-fold higher compared with TRPV5$^{+/+}$ cultures (Fig. 4 *A*, *B*, and *E*). Moreover, the number of nuclei per osteoclast was significantly increased in TRPV5$^{-/-}$ osteoclasts compared with TRPV5$^{+/+}$ osteoclasts (Fig. 4 *B* and *F*). These data strongly support our *in vivo* findings (Fig. 3) that osteoclastogenesis is enhanced in TRPV5$^{-/-}$ mice. Despite their increased size, osteoclasts derived from TRPV5$^{-/-}$ bone marrow cells expressed similar levels of calcitonin receptor mRNA expression compared with TRPV5$^{+/+}$ osteoclasts (data not shown). In addition, with a fluorescent phalloidin-rhodamin antibody on mature TRPV5$^{+/+}$ and TRPV5$^{-/-}$ osteoclasts, both TRPV5$^{+/+}$ and TRPV5$^{-/-}$ osteoclasts respond similarly to 10 nM human calcitonin as shown by loss of the actin ring staining within 10 min after addition (data not shown). These findings show that despite the absence of TRPV5 the osteoclasts respond normally to their major regulator of resorbing activity.

Subsequently, bone resorption was measured by a resorption pit assay based on osteoclasts derived from bone marrow cultures and seeded on cortical bone slices. In cultures of TRPV5$^{+/+}$ osteoclasts, resorption pits were clearly observed (Fig. 4*C*). However, in tibial bone marrow cultures of TRPV5$^{-/-}$ mice, bone resorption was diminished (Fig. 4 *D* and *G*). Taken together, our *in vivo* and *in vitro* findings demonstrated that bone resorption by osteoclasts lacking TRPV5 is severely impaired despite the presence of increased number and size of osteoclasts. The increase in the amount and size of osteoclasts suggests a compensatory mechanism to make up for the diminished osteoclast function. Next, we made an attempt to elucidate the mechanism of this presumed compensatory mechanism.

Diminished Resorption Does Not Enhance Osteoclastogenesis in TRPV5$^{-/-}$ Mice. It is generally accepted that an increase in ambient Ca^{2+} concentration sensed by the calcium-sensing receptor (CaSR) on osteoclast precursors (13, 14) inhibits osteoclast formation and/or function. Because bone resorption in the TRPV5$^{-/-}$ osteoclasts is diminished, unaltered Ca^{2+} levels may prevent CaSR activation, leading to the observed enhanced osteoclastogenesis. To explore this possibility, we examined TRPV5$^{+/+}$ and TRPV5$^{-/-}$ osteoclast formation on a plastic surface, thereby preventing resorption-induced changes in ambient Ca^{2+} levels. Similar to bone marrow cultures seeded on bone slices, osteoclast numbers in the TRPV5$^{-/-}$ cultures increased 2-fold (Fig. 5*A*), and elevated numbers of nuclei per osteoclast versus TRPV5$^{+/+}$ bone marrow cultures were observed (Fig. 5*B*). These data indicated that lack of resorption and release of Ca^{2+} did not cause the observed increased osteoclastogenesis in TRPV5$^{-/-}$ mice.

Elevated 1,25(OH)$_2$D$_3$ Levels in TRPV5$^{-/-}$ Mice Accelerate Osteoclastogenesis. Early studies showed that 1,25(OH)$_2$D$_3$ stimulates the formation of bone-resorbing osteoclasts from precursors or in cocultures of bone marrow cells and osteoblasts (15–18). Because TRPV5$^{-/-}$ mice have increased 1,25(OH)$_2$D$_3$ levels (7) and increased osteoclastogenesis *in vivo*, we assessed whether more osteoclast precursors exist in bone marrow of TRPV5$^{-/-}$ mice explaining the observed enhanced osteoclast formation. To this end, osteoclast numbers were determined at days 1 and 2 after initiation of bone marrow cultures, when rapid expansion of precursor cells toward TRACP-positive cells becomes manifest. The amounts of TRACP-positive cells were significantly elevated at

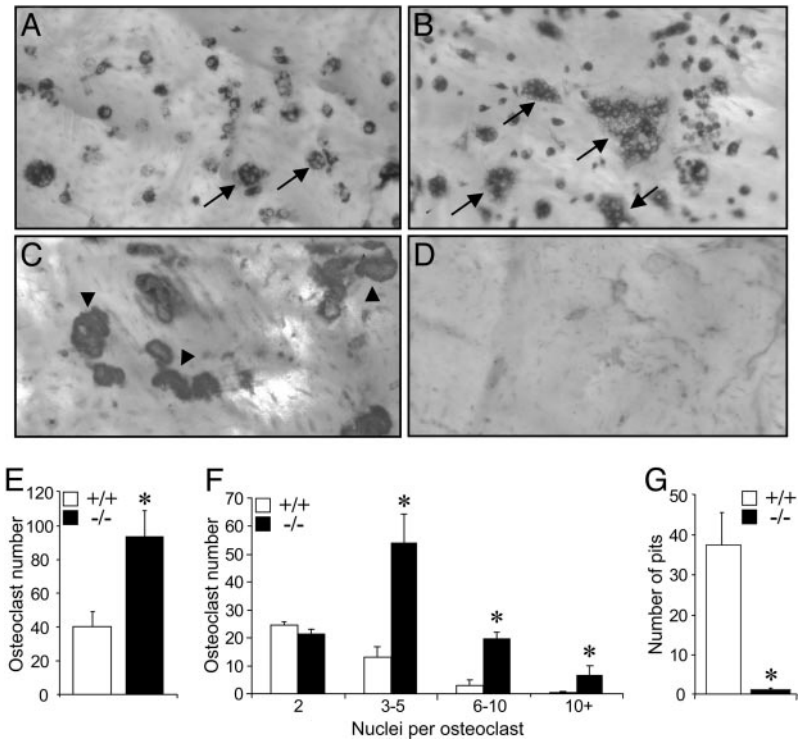

Fig. 4. Osteoclastogenesis *in vitro* is enhanced but resorption is diminished. (*A* and *B*) Murine bone marrow cells from TRPV5$^{+/+}$ (*A*) and TRPV5$^{-/-}$ (*B*) mice were cultured on bovine cortical bone slices for 6 days and stained for TRACP to visualize multinucleated osteoclasts. Arrows indicate multinuclear osteoclasts. (*C* and *D*) Coomassie brilliant blue was used to stain the resorption pits in TRPV5$^{+/+}$ (*C*) and TRPV5$^{-/-}$ (*D*) cultures. Arrowheads indicate resorption pits. (*E*–*G*) In these cultures, osteoclast number (*E*), the number of nuclei per osteoclast (*F*), and the number of resorption pits per bone slice (*G*) were quantified ($n = 6$–9). Values are presented as mean ± SEM. *, $P < 0.05$ versus TRPV5$^{+/+}$ cultures.

both time points in TRPV5$^{-/-}$ cultures (Fig. 6), thereby providing evidence for an increased number of osteoclast precursors in the bone marrow of mice lacking TRPV5. This finding indicates that there is an enhanced and/or accelerated osteoclast differentiation pathway in the presence of extreme high levels of 1,25(OH)$_2$D$_3$ in TRPV5$^{-/-}$ mice.

Osteoclast/Bone Phenotype in TRPV5$^{-/-}$ Mice. The findings in this study and our previous study (7) revealed that in TRPV5$^{-/-}$ mice two apparently opposite phenomena are evident: disturbed bone resorption and reduced bone thickness (Fig. 7). First, mice lacking TRPV5 display severely disturbed bone resorption as a consequence of malfunctional osteoclasts. In fact, it is intriguing why TRPV5$^{-/-}$ mice do not develop osteopetrosis. Patients harboring mutations in the genes encoding the vacuolar H$^+$-ATPase and the chloride channel CLC-7 develop autosomal dominant osteopetrosis (type II benign human osteopetrosis) as a result of absent acidification of the resorption lacunae, resulting in defective bone resorption (19, 20). In fact, in this condition osteoclast number is 3-fold increased (21). Similarly, in our study, TRPV5$^{-/-}$ mice also showed diminished bone resorption together with an increased number of osteoclasts. Despite these phenomena, no osteopetrotic phenotype (including increased cartilage remnants in the secondary spongiosa; data not shown) is observed and there is even a reduction in bone thickness (7) in mice lacking TRPV5.

First, regarding an osteopetrotic phenotype it is of interest that TRPV5 and TRPV6 have been shown to form homotetramers and heterotetramers *in vitro* and are highly selective for Ca^{2+} (22).

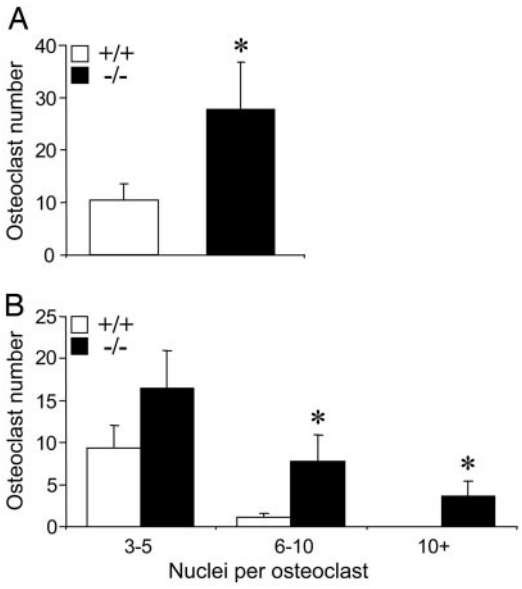

Fig. 5. Diminished resorption does not enhance osteoclastogenesis in TRPV5$^{-/-}$ mice. Murine bone marrow cells from TRPV5$^{+/+}$ and TRPV5$^{-/-}$ mice were cultured on plastic instead of cortical bone slices for 6 days and stained for TRACP. The amount of osteoclasts (*A*) and the number of nuclei per osteoclast (*B*) was measured for both cultures ($n = 6$). Values are presented as mean ± SEM. *, $P < 0.05$ versus TRPV5$^{+/+}$ cultures.

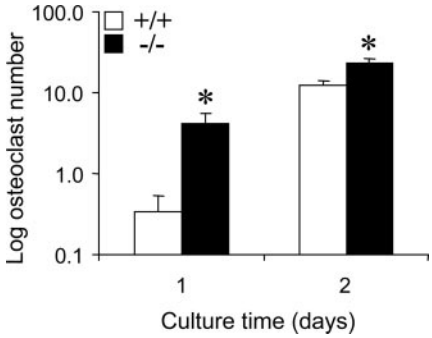

Fig. 6. Increased number of osteoclast precursors in TRPV5$^{-/-}$ mice. Murine bone marrow cells from TRPV5$^{+/+}$ and TRPV5$^{-/-}$ mice were cultured on plastic and stained for TRACP at days 1 and 2 of culture. The number of TRACP-positive cells was quantified ($n = 6$). Values are presented as mean ± SEM. *, $P < 0.05$ versus TRPV5$^{+/+}$ cultures.

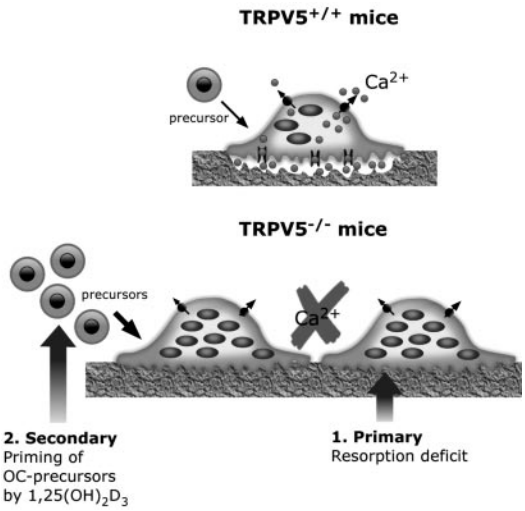

Fig. 7. Osteoclast phenotype in TRPV5$^{-/-}$ mice. The findings in this study reveal two phenomena, which contribute to the osteoclast phenotype in TRPV5$^{-/-}$ mice. First, an intrinsic defect occurs in TRPV5$^{-/-}$ osteoclasts, leading to a bone resorption deficit, as opposed to TRPV5$^{+/+}$ mice. Second, priming of bone marrow by high $1,25(OH)_2D_3$ levels may result in more osteoclast precursors in TRPV5$^{-/-}$ compared with TRPV5$^{+/+}$ mice, leading to an increase in the amount and size of osteoclasts.

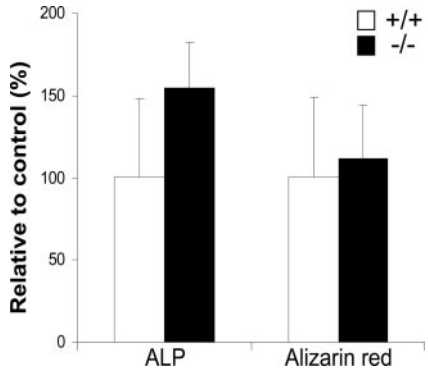

Fig. 8. Osteoblast differentiation is not altered in TRPV5$^{-/-}$ mice. Murine bone marrow cells from TRPV5$^{+/+}$ and TRPV5$^{-/-}$ mice were either cultured for 10 days and stained for ALP or cultured for 20 days and stained for mineralization (alizarin red). The number of ALP- and alizarin red-positive colonies were quantified. Values are presented as mean ± SD.

Because TRPV6 is also expressed in osteoclasts (data not shown), it might in homotetramer form at least partly compensate for the absence of TRPV5 channels explaining the absence of an osteopetrotic phenotype. In contrast, intestine TRPV6 expression in osteoclasts derived from bone marrow TRPV5$^{-/-}$ mice appeared not to be increased compared with WT osteoclasts potentially explaining the lack of full compensation of the diminished bone resorption.

Second, the high $1,25(OH)_2D_3$ level found in these mice may be related to the observed bone phenotype. Despite the antirachitic nature of $1,25(OH)_2D_3$ in humans, several reports show it in mice to be negatively correlated to bone thickness. First, vitamin D receptor-ablated mice have increased cortical bone thickness (23), and show excessive bone formation in a normal mineral condition (24). Interestingly, long-term treatment of mice with $1,25(OH)_2D_3$ displayed a decrease in cortical thickness and cross-sectional area, but also a 50% reduction in stiffness (25). Moreover, $1,25(OH)_2D_3$ treatment of murine osteoblasts inhibits the development of a fully mature osteoblastic phenotype as well as matrix mineralization (26). Therefore, the role of $1,25(OH)_2D_3$ in this study in relation to the bone phenotype in our previous study (7) is explained either by increased resorption or reduced formation. Because increased resorption is unlikely as shown by this study, reduced bone formation is probably involved. We investigated osteoblast function *in vitro* by culturing bone marrow-derived osteoblasts from both WT and TRPV5$^{-/-}$ mice for 3 weeks and stained for ALP and mineralization. WT and TRPV5$^{-/-}$ osteoblast cultures contain similar amounts of ALP- and alizarin red-positive osteoblast colonies (Fig. 8), showing that osteoblast differentiation is not intrinsically disturbed in mice lacking TRPV5. Nevertheless, because TRPV5 is exclusively expressed in osteoclasts, diminished osteoclast function may *in vivo* lead via an altered coupling to reduced bone formation. However, on the basis of serum osteocalcin and ALP level in TRPV5$^{-/-}$ mice (7) this assumption is not clear yet. Alternatively, in TRPV5$^{-/-}$ mice, less Ca^{2+} may be available for bone formation, as it is needed for maintenance of serum Ca^{2+}. Further studies are obviously needed to unravel the precise relationship between $1,25(OH)_2D_3$ and bone thickness.

In conclusion, we have shown that TRPV5 and other transcellular Ca^{2+} transporters are expressed in human and murine osteoclasts and that TRPV5 is an essential Ca^{2+} transporter in osteoclastic bone resorption. Thus, alterations in TRPV5 function will likely have implications for metabolic bone diseases and forwards it as a possible target for therapeutic interventions.

We thank Dr. H. Jahr (Erasmus Medical Center) for providing cDNAs from human bone biopsies and M. Koedam for technical assistance. This work was supported by Dutch Organization of Scientific Research Grants Zon-Mw 902.18.298 and Zon-Mw 016.006.001 and Dutch Kidney Foundation Grant C03.6017.

1. Hoenderop, J. G. & Bindels, R. J. (2005) *J. Am. Soc. Nephrol.* **16,** 15–26.
2. Bronner, F. (1998) *J. Nutr.* **128,** 917–920.
3. Hoenderop, J. G., Van Der Kemp, A. W., Hartog, A., van de Graaf, S. F., Van Os, C. H., Willems, P. H. & Bindels, R. J. (1999) *J. Biol. Chem.* **274,** 8375–8378.
4. Peng, J. B., Chen, X. Z., Berger, U. V., Vassilev, P. M., Tsukaguchi, H., Brown, E. M. & Hediger, M. A. (1999) *J. Biol. Chem.* **274,** 22739–22746.
5. Montell, C., Birnbaumer, L., Flockerzi, V., Bindels, R. J., Bruford, E. A., Caterina, M. J., Clapham, D. E., Harteneck, C., Heller, S., Julius, D., *et al.* (2002) *Mol. Cell* **9,** 229–231.
6. Hoenderop, J. G., Nilius, B. & Bindels, R. J. (2005) *Physiol. Rev.* **85,** 373–422.
7. Hoenderop, J. G., van Leeuwen, J. P., van der Eerden, B. C., Kersten, F. F., Van Der Kemp, A. W., Merillat, A. M., Waarsing, J. H., Rossier, B. C., Vallon, V., Hummler, E., *et al.* (2003) *J. Clin. Invest.* **112,** 1906–1914.
8. de Vries, T. J., Schoenmaker, T., Beertsen, W., van der Neut, R. & Everts, V. (2005) *J. Cell Biochem.* **94,** 954–966.
9. Derkx, P., Nigg, A. L., Bosman, F. T., Birkenhager-Frenkel, D. H., Houtsmuller, A. B., Pols, H. A. & van Leeuwen, J. P. (1998) *Bone* **22,** 367–373.
10. Eijken, M., Hewison, M., Cooper, M. S., de Jong, F. H., Chiba, H., Stewart, P. M., Uitterlinden, A. G., Pols, H. A. & van Leeuwen, J. P. (2005) *Mol. Endocrinol.* **19,** 621–631.
11. Hoenderop, J. G., Hartog, A., Stuiver, M., Doucet, A., Willems, P. H. & Bindels, R. J. (2000) *J. Am. Soc. Nephrol.* **11,** 1171–1178.
12. Scheven, B. A., Kawilarang-De Haas, E. W., Wassenaar, A. M. & Nijweide, P. J. (1986) *Anat. Rec.* **214,** 418–423.
13. Kanatani, M., Sugimoto, T., Kanzawa, M., Yano, S. & Chihara, K. (1999) *Biochem. Biophys. Res. Commun.* **261,** 144–148.
14. Shin, M. M., Kim, Y. H., Kim, S. N., Kim, G. S. & Baek, J. H. (2003) *Exp. Mol. Med.* **35,** 167–174.
15. Tinkler, S. M., Linder, J. E., Williams, D. M. & Johnson, N. W. (1981) *J. Anat.* **133,** 389–396.
16. Roodman, G. D., Ibbotson, K. J., MacDonald, B. R., Kuehl, T. J. & Mundy, G. R. (1985) *Proc. Natl. Acad. Sci. USA* **82,** 8213–8217.
17. Takahashi, N., Akatsu, T., Udagawa, N., Sasaki, T., Yamaguchi, A., Moseley, J. M., Martin, T. J. & Suda, T. (1988) *Endocrinology* **123,** 2600–2602.
18. Takahashi, N., Yamana, H., Yoshiki, S., Roodman, G. D., Mundy, G. R., Jones, S. J., Boyde, A. & Suda, T. (1988) *Endocrinology* **122,** 1373–1382.
19. Frattini, A., Orchard, P. J., Sobacchi, C., Giliani, S., Abinun, M., Mattsson, J. P., Keeling, D. J., Andersson, A. K., Wallbrandt, P., Zecca, L., *et al.* (2000) *Nat. Genet.* **25,** 343–346.
20. Cleiren, E., Benichou, O., Van Hul, E., Gram, J., Bollerslev, J., Singer, F. R., Beaverson, K., Aledo, A., Whyte, M. P., Yoneyama, T., *et al.* (2001) *Hum. Mol. Genet.* **10,** 2861–2867.
21. Bollerslev, J., Marks, S. C., Jr., Pockwinse, S., Kassem, M., Brixen, K., Steiniche, T. & Mosekilde, L. (1993) *Bone* **14,** 865–869.
22. Hoenderop, J. G., Voets, T., Hoefs, S., Weidema, F., Prenen, J., Nilius, B. & Bindels, R. J. (2003) *EMBO J.* **22,** 776–785.
23. Amling, M., Priemel, M., Holzmann, T., Chapin, K., Rueger, J. M., Baron, R. & Demay, M. B. (1999) *Endocrinology* **140,** 4982–4987.
24. Tanaka, H. & Seino, Y. (2004) *J. Steroid Biochem. Mol. Biol.* **89–90,** 343–345.
25. Smith, E. A., Frankenburg, E. P., Goldstein, S. A., Koshizuka, K., Elstner, E., Said, J., Kubota, T., Uskokovic, M. & Koeffler, H. P. (2000) *J. Endocrinol.* **165,** 163–172.
26. Fratzl-Zelman, N., Glantschnig, H., Rumpler, M., Nader, A., Ellinger, A. & Varga, F. (2003) *Cell Biol. Int.* **27,** 459–468.